Electronic Supplementary Material (ESI) for Soft Matter.


# Supporting Information

## Spontaneous penetration mechanism of patterned nanoparticles across a biomembrane

Ye Li, Xianren Zhang and Dapeng Cao

*State Key Laboratory of Organic-Inorganic Composites, Beijing University of Chemical Technology, Beijing 100029, China*

Table S1 The number of times of independent simulation runs and the reproducibility of our results.

| Figure | The number of times | Reproducibility |
|---|---|---|
| Fig. 2 | Three times for, respectively, 3-SNP (26%), 3-SNP (42%) and 3-SNP (80%). | For 3-SNP (26%), all simulation runs show successful penetrations with a penetration-rotation mechanism.<br>For 3-SNP (42%) and 3-SNP (80%), all simulation runs fail to achieve NP penetrations. |
| Fig. 4 | Three times for, respectively, 3-SNP (D=3.23), 3-SNP (4.52), 3-SNP (5.81) and 3-SNP (11.0).<br>Three times for, respectively, 3-SNP ($\lambda = 32.2$ %), 3-SNP (23.6%), 3-SNP (10.2 %), and 3-SNP (5.6 %). | For 3-SNP (3.23nm), 3-SNP (4.52nm), and 3-SNP (5.6%), all simulation runs show successful penetrations.<br>For 3-SNP (5.81nm), 3-SNP (11.0nm), 3-SNP (32.2%), 3-SNP (23.6 %) and 3-SNP (10.2 %), all simulation runs fail to achieve NP penetrations. |
| Fig. 5 | Three times for, respectively, 3-SNP (7.1nm), 5-SNP (7.1nm), 16-SNP (7.1nm), 3-SNP (11.0nm), 5-SNP (11.0nm) and 26-SNP (11.0nm). | For 5-SNP (7.1nm), 16-SNP (7.1nm) and 26-SNP (11.0nm), all simulation runs show successful penetrations.<br>For 3-SNP (7.1nm), 3-SNP (11.0nm) and 5-SNP (11.0nm), all simulation runs fail to achieve NP penetrations. |
| Fig. 6 | Three times for 16-SNP (7.1). | All simulation runs show successful penetrations. |
| Fig. 7 | Three times for, respectively, 4-PNP (7.1nm), 6-PNP (7.1nm), RNP (7.1nm), 4-PNP (11.0nm), 6-PNP (11.0nm) and RNP (11.0nm). | For 6-PNP (7.1nm), 6-PNP (11.0nm), RNP (7.1nm) and RNP (11.0nm) all simulation runs show successful penetrations.<br>For 4-PNP (7.1nm) and 4-PNP (11.0nm) all simulation runs fail to achieve NP penetrations. |
| Fig. 9/10 | Three times for, respectively, 3-SNP (13.75nm), 16-SNP (13.75nm), 3-SNP (6.25nm) and 7-SNP (6.25nm). | For different NPs, all simulation runs show successful NP penetrations and NP aggregations.<br>For 16-SNP (13.75nm), 3-SNP (6.25nm) and 7-SNP (6.25nm), all simulation runs did not show solvent leakage.<br>For 3-SNP (13.75nm) and $N_{np}$=30, the formation of the hydrophilic pore was found in one of the three runs, while in the other runs the transient hydrophobic pores were observed instead. |

Table S2 Penetrability of different patterned NPs with $\lambda$=50% across a membrane.

| Penetration | 5-SNP (7.1nm) | 16-SNP (7.1 nm) | 16-SNP (11nm) | 6-PNP (7.1nm) | 6-PNP (11.0nm) | RNP (7.1nm) | RNP (11.0nm) |
|---|---|---|---|---|---|---|---|
| Non-penetration | 3-SNP (7.1nm) | 3-SNP (11.0nm) | 5-SNP (11nm) | 4-PNP (7.1nm) | 4-PNP (11.0nm) | | |

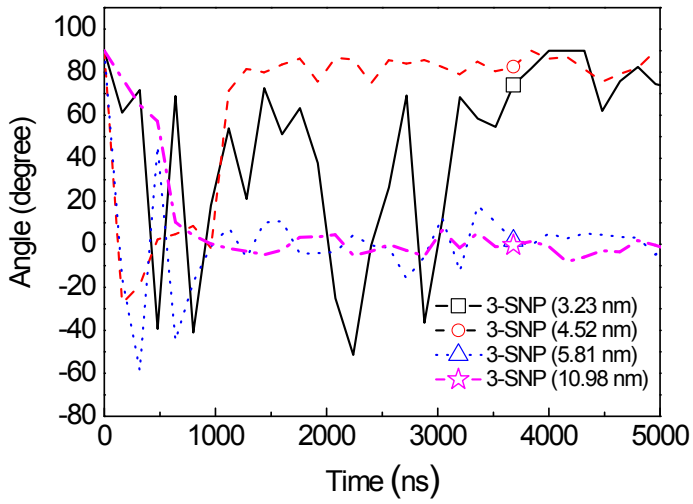


Fig. S1. Time evolution of the orientation of 3-SNPs during their penetration processes. Note that $\lambda \approx$32.2% as in the Fig. 4.

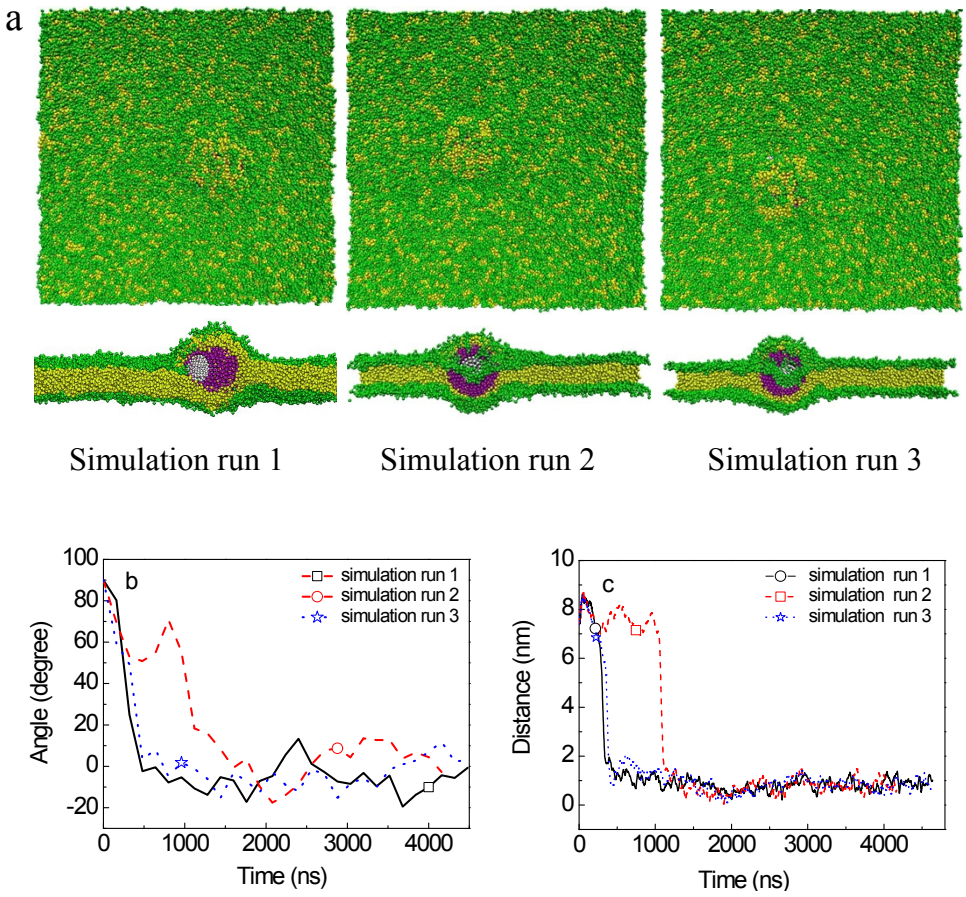


Fig. S2. Penetration processes for 3-SNPs with D=11nm and $\lambda$=10.2% obtained from three independent simulation runs. (a) Final configurations after a simulation run of 6400 ns. (b,c) show the time evolution of the NP orientation (b) and NP-bilayer distance (c). The color code for the snapshots is the same as in Fig. 1.

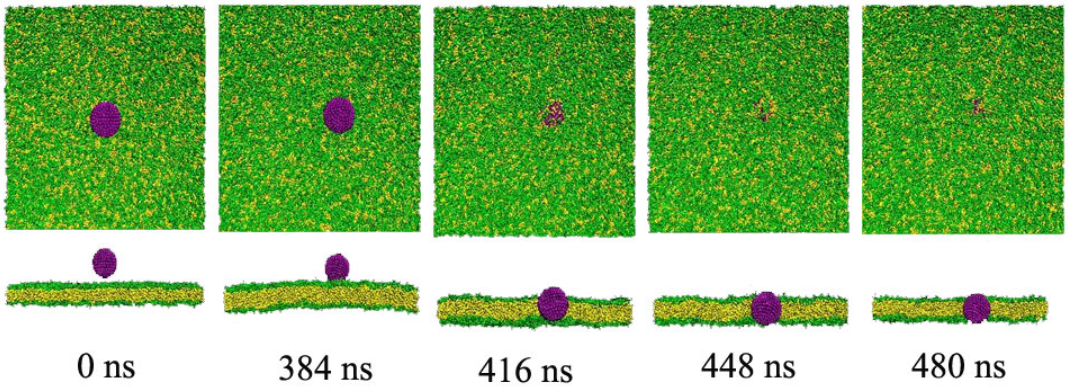


Fig. S3. Typical configurations for the penetration of a hydrophobic NP ($\lambda$=0%) of 7.1 nm during its penetration process.

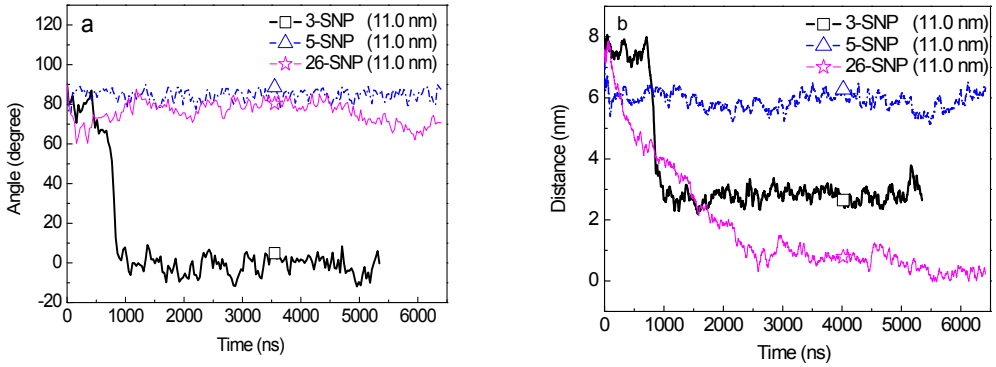


Fig. S4. (a) Time evolution of the SNP ($\lambda$=50%) orientation. (b) Time evolution of the distance between the NP center and the bilayer center during the penetration of large SNPs ($\lambda$=50%) of 11.0 nm across a flat membrane.

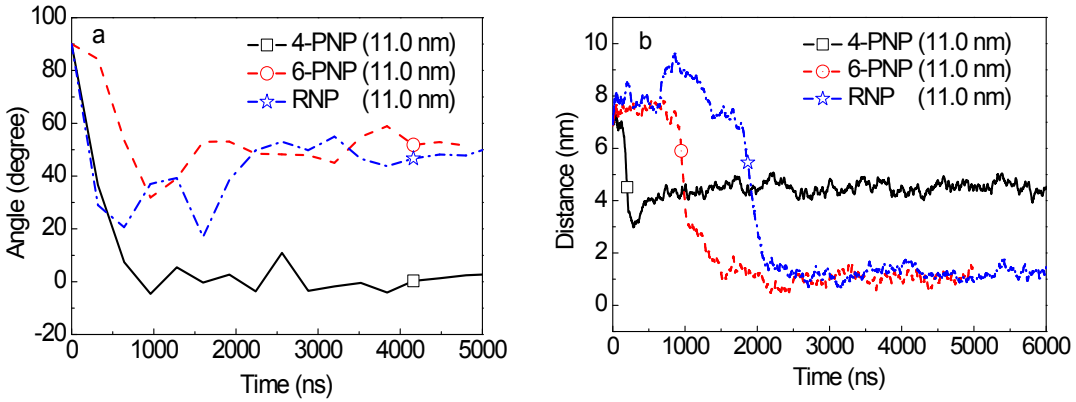


Fig. S5. (a) Time evolution of the NP orientation angle during the penetration process for PNPs ($\lambda$=50%) and RNPs ($\lambda$=50%). (b) Time evolution of the distance between the NP center and the bilayer center for PNPs ($\lambda$=50%) and RNPs ($\lambda$=50%).

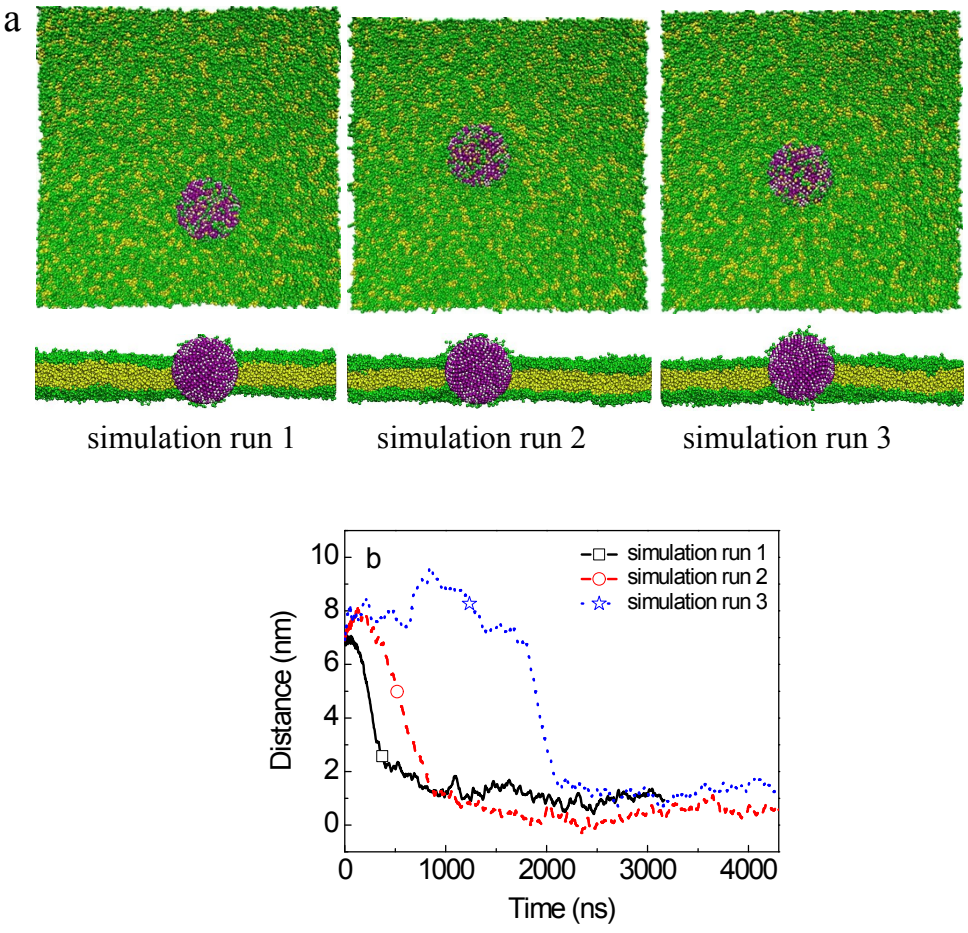


Fig. S6. Penetration of RNPs with D=11.0nm and $\lambda$=50% obtained from three independent simulation runs. (a) Final configurations after a simulation run of 6400 ns. The color code for the snapshots is the same as in Fig. 1. (b) shows the time evolution of NP-bilayer distance.

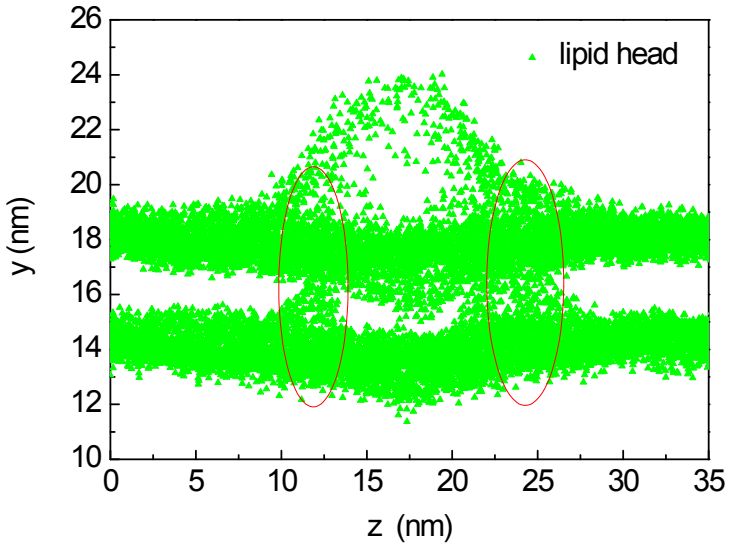


Fig. S7. The distribution of the lipid heads for the system with a 3-SNP of 11.0 nm ( $\lambda \approx 32.2\%$ ).The lipid heads into the membrane hydrophobic core in red circle.

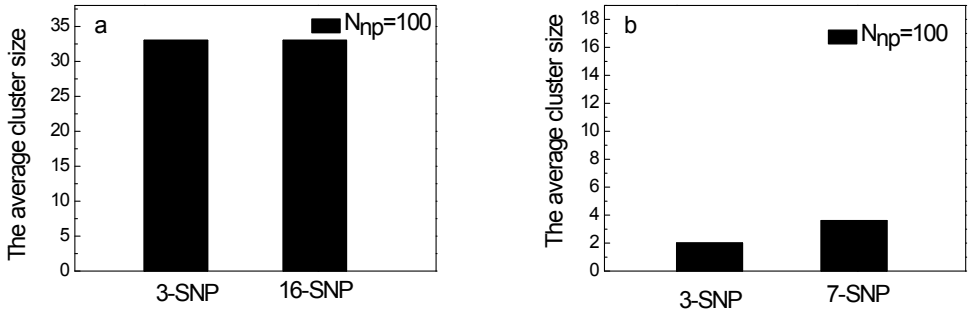


Fig. S8. The average cluster size (a) for 3-SNPs and 16-SNPs having a diameter of 13.75 nm and for (b) 3-SNPs and 7-SNPs with a diameter of 6.25 nm.

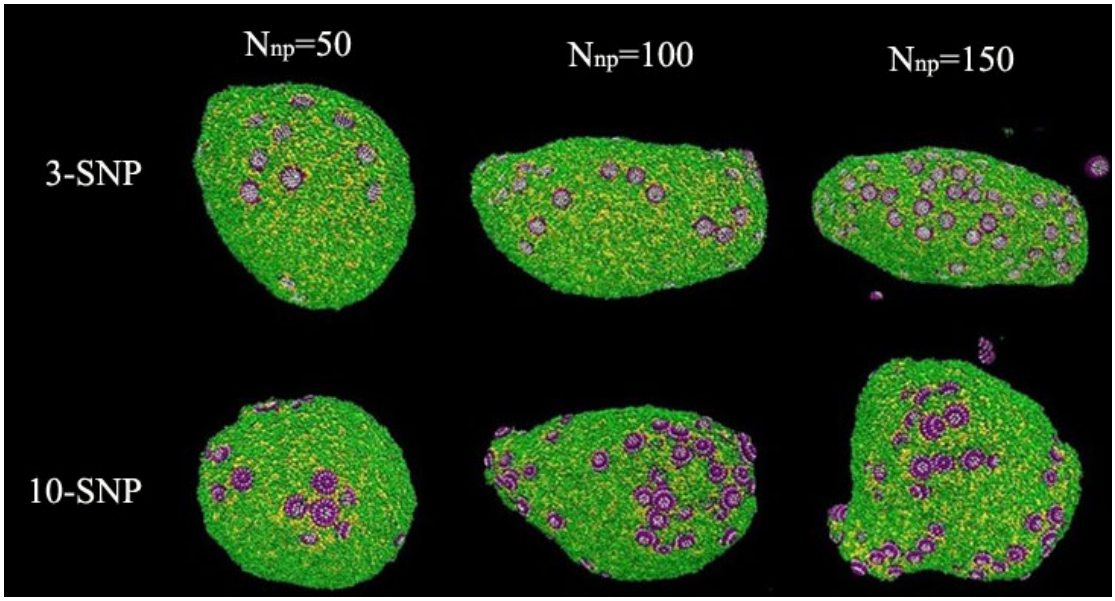


Fig. S9. Typical snapshots after the penetration of n-SNPs across the vesicle membrane. The NP diameters in this figure were set to 8.75 nm. The color code for the snapshots is the same as in Fig.1.

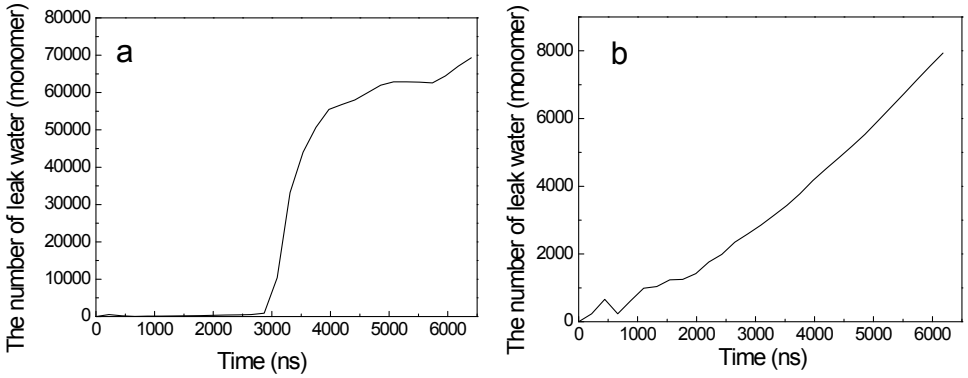


Fig. S10. (a) Time evolution of the number of leak solvent (3-SNP (D=13.75 nm, $N_{np}$ =30)). (b) Time evolution of the number of leak solvent 3-SNP (D=13.75 nm, $N_{np}$ =50)).